European Review for Medical and Pharmacological Sciences 2018; 22: 135-141

Correlation of CT indicators of NSCLC and pathological features and the expression level of p53 and c-myc

H.-S. LI[1], R.-Q. LV[2], L. LIU[3]

[1]Imaging Department, Linyi Central Hospital, Shandong, China
[2]Laboratory Medicine, People's Hospital of Juxian, Shandong, China
[3]Respiratory Medicine, Shanxian County Central Hospital of Shandong Province, Shandong, China

Hongsong Li and Ruiqi Lv contributed equally to this work

Abstract. – OBJECTIVE: To investigate the correlations of the computed tomography (CT) signs of non-small cell lung cancer (NSCLC) with pathological features and the expression levels of phosphoprotein 53 (p53) and c-Myc in patients.

PATIENTS AND METHODS: 87 patients with NSCLC admitted to the Department of Oncology in our hospital from July 2014 to March 2017 were randomly selected. Morphologies of NSCLC and cancer-adjacent tissues were detected by hematoxylin and eosin (H&E) staining; messenger ribonucleic acid (mRNA) and protein levels of p53 and c-Myc in cancer and cancer-adjacent tissues were detected using real-time polymerase chain reaction (RT-PCR) and immunohistochemistry (IHC); spiral CT (SCT) was conducted for exploring imaging signs of patients with NSCLC; the correlation of CT signs with pathology and the expressions of p53 and c-Myc was analyzed.

RESULTS: H&E staining showed that NSCLC tissues had a larger nucleus, a larger nucleus-cytoplasm ratio, and a more evident histopathological atypia, with no clear histological structure compared with cancer-adjacent normal tissues; RT-PCR and IHC results revealed that the mRNA and protein expression levels of p53 and c-Myc in NSCLC tissues were significantly higher than those in cancer-adjacent tissues, in which differences in mRNA levels were 1.75 folds and 1.84 folds, respectively ($p<0.05$). SCT signs indicated that swollen lymph nodes and spiculation, spinous process and deep lobulation signs often occurred in the chest of NSCLC patients, and pleural indentation appeared in the majority of patients; the chi-square test results showed that the positive rates of p53 and c-Myc proteins were not related to pathological types of NSCLC, but significantly correlated with tumor differentiation ($p<0.05$); the positive rates of p53 and c-Myc proteins were correlated with tumor diameter, spiculation and deep lobulation signs and lymph node metastasis ($p<0.05$), but not associated with spinous process, vacuole and pleural indentation signs ($p>0.05$).

CONCLUSIONS: CT scan combined with the detection of p53 and c-Myc expressions can improve the diagnosis of lymph node metastasis and clinical staging for patients with NSCLC, which is conducive to the clinical treatment and prognosis analysis of NSCLC.

Key Words
NSCLC, Spiral CT, p53, c-Myc.

Introduction

Lung cancer is one of the major causes of death in patients, in which non-small cell lung cancer (NSCLC) accounts for about 80% of patients with bronchial lung cancer[1]. Large-scale screening has greatly improved the early diagnosis and treatment of lung cancer since the Early Lung Cancer Action Plan (ELCAP) was launched in the 1990s. The results of this action showed that spiral computed tomography (SCT) can be used to identify individuals with high risk of early-stage lung cancer in a very small size, and the accurate diagnosis rate for Stage I tumors is more than 80%[2]. Therefore, SCT is an effective method both in the early intervention and in the screening of high-risk groups of lung cancer. Tumor suppressor gene phosphoprotein 53 (p53) mutant and its downstream oncogene c-Myc are commonly seen in a variety of human tumors, and at present, they are indicators used in clinical tumor diagnosis and staging[3,4]. However, there is no report on whether CT imaging signs combined with p53 and c-Myc expressions improve the diagnosis and prognosis of NSCLC in relevant literature.

Corresponding Author: Lei Liu, MD; e-mail: i6s140@163.com

The primary purpose was to investigate the correlations of computed tomography (CT) signs of non-small cell lung cancer (NSCLC) with pathological features and the expression levels of phosphoprotein 53 (p53) and c-Myc in patients.

Patients and Methods

Clinical Data

A total of 87 patients admitted to the Department of Oncology in our hospital from July 2014 to March 2017 were randomly selected. The patients were at the average age of (53.4±6.7) years old, and they underwent full-body CT development before the operation. There were no significant differences in general clinical data among the included patients. Specimens came from surgical resection or pathologic biopsy. Data of hematoxylin and eosin (H&E) staining and SCT were evaluated by three different physicians from the Pathology Department and the Imaging Department, respectively. Imaging and histopathological detection results were compared among all the cases. The study was approved by the Ethics Committee of Shanxian County Central Hospital of Shandong Province, and all the patients signed the written informed consent.

Detection of NSCLC Pathological Condition Using SCT

The double SCT (CT-Twin, Elscint Ltd., Haifa, Israel) was applied for scans, and a 512×512 matrix was reconstructed. The layer thickness and spacing were 10 mm, and 5 mm thin layer in the lesion area was scanned additionally. Besides, high-resolution CT (HRCT) scan was used in the lesion area of some patients. CT signs were summarized by conventional CT findings.

Detection of the Messenger Ribonucleic Acid (mRNA) levels of p53 and c-Myc in NSCLC Tumor Tissues by Real-time Polymerase Chain Reaction (RT-PCR)

The total RNA was extracted from NSCLC tissues using TRIzol reagents, and 1 μg total RNA was reversely transcribed using Reverse Transcription Kit (Article Number: 205311, Qiagen, Grindelwald, NY, USA). RT-PCR was conducted using the SYBR® Premix Ex Taq™ II Kit (Takara, Tokyo, Japan). 45 cycles of amplification were performed at an annealing temperature of 55°C. The relative quantification of each gene was analyzed by $2^{-\Delta Ct}$ with glyceraldehyde-3-phosphate dehydrogenase (GAPDH) as the internal reference for correction. The relative mRNA expression level of each gene was calculated as $2^{-\Delta Ct}$ [ΔCt = Ct (target gene) – Ct (GAPDH)]. Primer sequences are listed below: p53 exonic primers: Forward in exon 5-9, 5'-GCCGTGTTCCAGTTGCTTTATCTGTTCAC-3', Reverse in exon 15028-14998, 5'-GTGTTGTCTCCTAGGTTGGCTCTG-3'; c-Myc: Forward, 5'-CTTGTCCTCCTTTCTGTTACGG-3', Reverse, 5'-CCCCTGTAGCCATCCATTCC-3'; GAPDH: Forward, 5'-ATTGATGGATGCTAFGAGTATT-3', Reverse, 5'-AGTCTTCTGGGTGGCAGTGAT-3'; each experiment was repeated for three times.

Observation of the Histomorphology by H&E Staining and Detection of the Protein Levels of p53 and c-Myc in Tumor and Tumor-adjacent Tissues by Immunohistochemistry (IHC)

87 cases of NSCLC specimens were fixed with 4% formaldehyde, followed by conventional dehydration and embedding into paraffin blocks, which were sliced into pieces at a thickness of 4 μm. Eosin and hematoxylin were used for H&E staining, respectively, followed by histopathological observation. Pathologically confirmed NSCLC and cancer-adjacent (4 cm or more) tissues were serially sectioned at 4 μm for IHC staining of p53 and c-Myc. In IHC technology, the two-step universal kit (Zhongshan Golden Bridge Biotechnology, Beijing, China, model: ZLl9610) was used, primary antibodies, p53, and c-Myc were purchased from RD Company (Minneapolis, MN, USA. Article Number: AF1355 and MAB3696), and secondary antibodies were labeled by diaminobenzidine (DAB) development. The known positive tissues were taken as the positive control, while phosphate-buffered saline (PBS), instead of primary antibodies, was regarded as the negative control. The appearance of tan areas in the cell nucleus or cytoplasm was defined as positive cells. Based on the Trans classification method, the patients were divided into 4 grades according to the color intensity and the number of positive cells: "+" "++" and "+++" represented positive, while "-" represented negative[5].

Statistical Analysis

The experimental results were analyzed using GraphPad Prism software (Version 5.01, GraphPad Software, Santiago de Chile, CA, USA). The chi-square test was used to compare the correlations of the levels p53 and c-Myc with pathological indicators and CT signs of NSCLC patients.

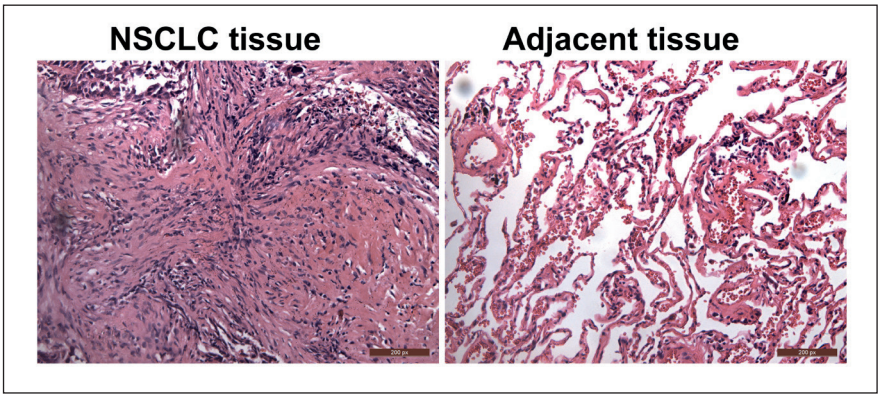

Figure 1. Detection of NSCLC and cancer-adjacent histomorphology by hematoxylin and eosin (H&E) staining. (Magnification: 40×)

The independent samples *t*-test was used to compare the differences in indicators between the two groups of specimens. $p<0.05$ represented that the difference was statistically significant.

Results

Detection of NSCLC and Cancer-adjacent Histomorphology by H&E

As shown in Figure 1, NSCLC tissues had larger nuclei, larger nucleus to cytoplasm ratio and more obvious histopathological atypia, with no clear organizational structure compared with those of cancer-adjacent normal tissues.

Detection of the Expressions of p53 and c-Myc by RT-PCR and IHC

As shown in Figure 2B, the mRNA expressions of p53 and c-Myc in NSCLC tissues were significantly higher than those in cancer-adjacent tissues, and the differences were 1.75 folds and 1.84 folds, respectively ($p<0.05$). IHC results (Figure 2A) revealed that p53 was expressed in the nucleus, while c-Myc was expressed in the cytoplasm. The protein levels of p53 and c-Myc in NSCLC tissues were significantly higher than those in cancer-adjacent tissues.

Correlation of p53 and c-Myc Levels with Pathological Indicators of NSCLC Patients

According to the Trans classification method, 34 patients were defined as p53-positive and 39 patients were defined as c-Myc-positive. The chi-square test results showed that the positive rates of p53 and c-Myc proteins were not related to pathological types of NSCLC, but significantly correlated with tumor differentiation ($p<0.05$) (Table I).

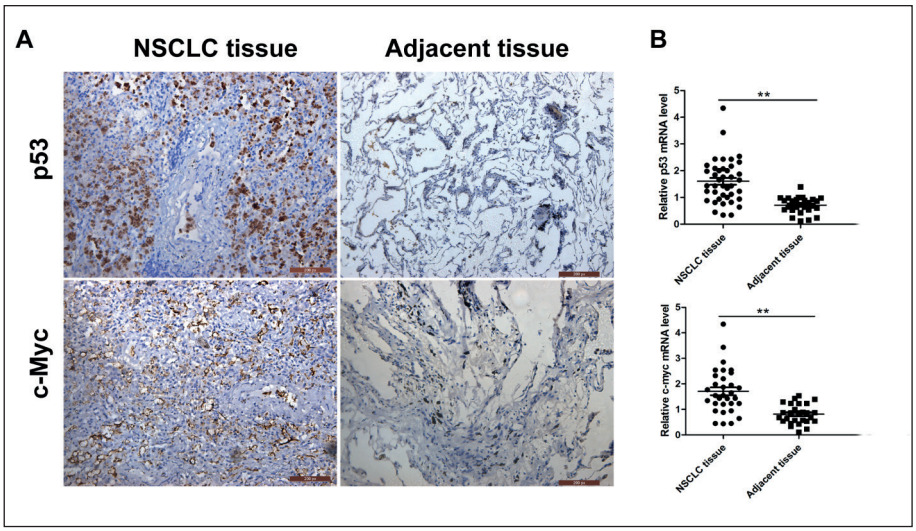

Figure 2. Detection of the expressions of p53 and c-Myc by RT-PCR and IHC. A, IHC suggests that p53 is expressed in the nucleus and c-Myc is expressed in the cytoplasm. The protein levels of p53 and c-Myc in NSCLC tissues are significantly higher than those in cancer-adjacent tissues. B, RT-PCR results show that the mRNA expressions of p53 and c-Myc in NSCLC tissues are significantly higher than those in cancer-adjacent tissues.

Table I. Correlation of the protein levels of p53 and c-Myc in NSCLC tissues with pathological.

Pathological feature		No.	p53		*p*-value	c-Myc		*p*-value
		87	Negative (53)	Positive (34)		Negative (48)	Positive (39)	
Pathological type	Squamous cell carcinoma	43	25	18	0.083	32	11	0.061
	Adenocarcinoma	28	19	9		12	16	
	Large-cell lung carcinoma	16	9	7		4	12	
Tumor differentiation	High differentiation	23	17	5	0.009	19	4	0.024
	Moderate differentiation	40	24	16		21	19	
	Low differentiation	24	12	12		8	16	

CT Signs of the Tumor in NSCLC Patients

SCT signs indicated that swollen lymph nodes and spiculation, spinous process and deep lobulation signs often occurred in the chest of NSCLC patients, and pleural indentation appeared in the majority of patients (Figure 3 and Table II).

Correlation of the Expressions of p53 and c-Myc with CT Signs of NSCLC Patients

The correlation of CT signs with the expressions of p53 and c-Myc was further explored by the chi-square test. The results showed that the positive rates of p53 and c-Myc proteins were correlated with tumor diameter, spiculation and deep lobulation signs and lymph node metastasis ($p<0.05$), but not associated with spinous process, vacuole and pleural indentation signs ($p>0.05$).

Correlation of the Expressions of p53 and c-Myc with Enhanced CT of NSCLC

As shown in Table III, the positive expressions of p53 and c-Myc in cancer tissues of patients with NSCLC were significantly correlated with the enhanced CT ($p<0.05$).

Discussion

Tumor suppressor gene p53 is the master gene regulator of many cellular pathways by activating or repressing downstream genes[6]. Among these genes, proto-oncogene c-Myc is negatively regulated by p53[7]. c-Myc is a transcription factor that directly or indirectly regulates a variety of genes and plays an important role in cell development, differentiation, proliferation and apoptosis[8,9]. It is hard to detect wild-type p53 in normal tissues, while mutant

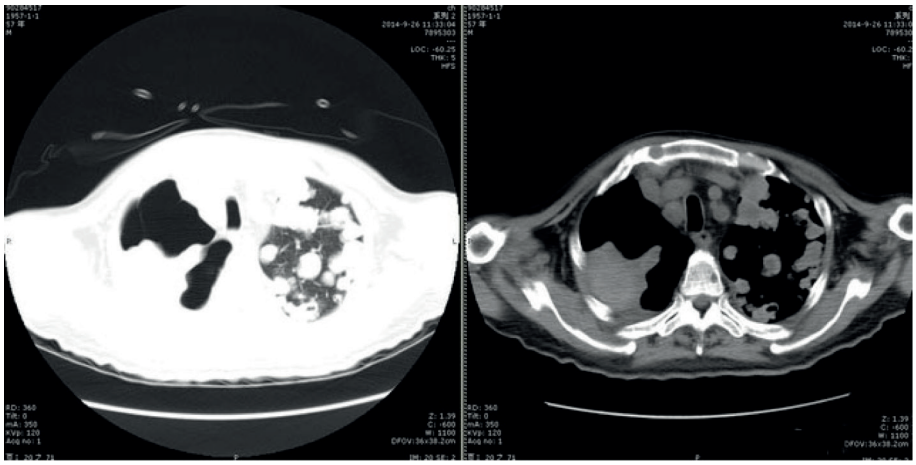

Figure 3. The NSCLC patient is a female aged 56 years old. CT signs suggest that nodules and lumps often occurred in patients at varying sizes and uneven density exist in the pleural cavity. Multiple mediastinal lymph nodes and fuzzy plaque shadows can be seen, which are considered as tumor metastasis accompanied with pulmonary infection.

Table II. Correlation of CT signs of NSCLC patients with the expressions of p53 and c-Myc.

Pathological feature		No.	p53		*p*-value	c-Myc		*p*-value
		87	Negative (53)	Positive (34)		Negative (48)	Positive (39)	
Diameter (cm)	≥3	53	30	23	0.042	36	17	0.015
	<3	34	23	11		12	22	
Spiculation sign	Yes	29	19	10	0.031	18	11	0.027
	No	58	34	24		30	28	
Spinouts process sign	Yes	43	29	14	0.172	27	12	0.306
	No	44	24	20		21	23	
Deep lobulation sign	Yes	46	32	24	0.024	31	15	0.039
	No	41	21	20		17	24	
Vacuole sign	Yes	31	24	7	0.047	15	16	0.617
	No	56	29	37		33	23	
Pleural indentation sign	Yes	49	25	24	0.295	27	22	0.072
	No	38	28	20		21	17	
Lymph node metastasis	Yes	50	36	14	0.017	39	11	0.036
		37	17	20		9	28	

p53 is often found in human tumor tissues. Mutant p53 loses its regulation of the oncogene c-Myc. In contrast, studies[10,11] have shown that the overexpressed c-Myc disrupts the p53-dependent G1/S cell cycle arrest caused by deoxyribonucleic acid (DNA) damages and promotes many cells to enter the cell cycle. Specifically, the overexpression of c-Myc disrupts G1 cyclin-dependent kinase inhibitors (p15, p16, P18, P19 and p27) after p53- and retinoblastoma protein (pRb)-associated growth arrest[12]. Currently, researchers have detected the expressions of c-Myc and mutant p53 in many human tumors such as breast cancer and colon cancer, which are often associated with aggressive and poorly differentiated tumors[13]. c-Myc is overexpressed in 30%-50% of the lung cancer patients[14]. In this experiment, IHC and RT-PCR were adopted, which showed that a large number of mutant p53 and c-Myc proteins were enriched in cancer tissues of NSCLC patients. It was found that the expressions of p53 and c-Myc were not associated with pathological types of NSCLC but significantly associated with NSCLC differentiation, which was consistent with Soucek's et al study[15].

Furthermore, SCT was used to detect the imaging signs of NSCLC patients, which showed that metastasis and deep lobulation, speculation, and spinous process signs often occurred in NSCLC patients. We found that CT signs of 50 patients with NSCLC showed lymph node metastasis, and 53 patients had tumors with a diameter greater than 3 cm. Besides, CT signs also showed that p53 and c-Myc were highly expressed in the tumor, which indicated that CT was of a certain value in detecting the size and metastasis of tumors, in which p53 and c-Myc were expressed. The lobulation sign is an appearance of multiple pronounced uneven arcs in the edge of tumors due to the different degrees of differentiation of tumor cells, where lobules with the chord length/chord length >2/5 are defined as deep lobules[16]. Spinous process sign, however, is considered as a type of lobulation sign with a thick and blunt "clubbing" structure, which is often infiltrated with NSCLC

Table III. Correlation of the expressions of p53 and c-Myc with the enhanced CT of NSCLC.

Detection index		No.	Enhanced SCT value		*p*-value
			>20 Hu	≤20 Hu	
p53	Negative	53	36	27	0.024
	Positive	34	26	18	
c-Myc	Negative	48	39	9	0.013
	Positive	39	25	14	

cells[17]. In this experiment, the sharp-pointed protrusions from the edge of the tumor to the lung observed in the mediastinum window edge occurred in the apex parts of tumor development area, representing that tumor cells were infiltrated in connective tissues around the blood vessels or spread along the lymphatic vessels. The spiculation sign is manifested as a lump with spine-like or spicule-like protrusions to varying degrees on the edge of the tumor, and squamous cell carcinoma can be manifested as long spicules, while adenocarcinoma is often manifested as short straight spicules[18]. We found that CT signs of NSCLC patients with highly expressed p53 and c-Myc were deep lobulation and spiculation sign, which might result from the formation of a scaffold due to the metastasis of NSCLC tumor cells to the surrounding tissues and distant areas, and this might be significantly correlated with the malignant biological behavior of the tumor and the poor prognosis of patients.

The primary cause of the formation of pleural indentation sign is the formation of intra-tumor reactive fibrosis and scars[19]. Although pleural indentation sign is a valuable indicator in the diagnosis of CT signs of lung cancer[20], this investigation showed that the expressions of p53 and c-Myc were not related to NSCLC patients with or without pleural indentation sign. Vacuole sign refers to a mini-focal photic zone in cancerous nodules shown in CT images with a diameter of less than 5 mm, which is distinguishable from cancerous voids. The smaller the diameter of the tumor is, the higher the incidence rate of vacuoles will be. The study revealed that the expressions of p53 and c-Myc in NSCLC were not related to vacuole sign, which was the same as the results of previous studies, indicating that vacuole sign was of little significance in judging the malignant biological behavior of NSCLC.

Conclusions

This study reveals that CT combined with the detection of p53 and c-Myc expressions can improve the diagnosis of lymph node metastasis and clinical staging for patients with NSCLC, which contributes to the clinical treatment and prognosis of NSCLC.

Conflict of Interest

The authors declared no conflict of interest.

References

1) Strauss GM, Herndon J, Maddaus MA, Johnstone DW, Johnson EA, Watson DM, Sugarbaker DJ, Schilsky RL, Green MR, Calgb F. Randomized Clinical Trial of adjuvant chemotherapy with paclitaxel and carboplatin following resection in Stage IB Non-Small Cell Lung Cancer (NSCLC): report of cancer and leukemia Group B (CALGB) Protocol 9633. J Clin Oncol 2004; 22: 7019.
2) Scagliotti G, Hanna N, Fossella F, Sugarman K, Blatter J, Peterson P, Simms L, Shepherd FA. The differential efficacy of pemetrexed according to NSCLC histology: a review of two Phase III studies. Oncologist 2009; 14: 253-263.
3) Felton-Edkins ZA, Kenneth NS, Brown TR, Daly NL, Gomez-Roman N, Grandori C, Eisenman RN, White RJ. Direct regulation of RNA polymerase III transcription by RB, p53 and c-Myc. Cell Cycle 2003; 2: 181-184.
4) Shi L, Wu YX, Yu JH, Chen X, Luo XJ, Yin YR. Research of the relationship between beta-catenin and c-myc-mediated Wnt pathway and laterally spreading tumors occurrence. Eur Rev Med Pharmacol Sci 2017; 21: 252-257.
5) Schonberger J, Ruschoff J, Grimm D, Marienhagen J, Rummele P, Meyringer R, Kossmehl P, Hofstaedter F, Eilles C. Glucose transporter 1 gene expression is related to thyroid neoplasms with an unfavorable prognosis: an immunohistochemical study. Thyroid 2002; 12: 747-754.
6) Riley T, Sontag E, Chen P, Levine A. Transcriptional control of human p53-regulated genes. Nat Rev Mol Cell Biol 2008; 9: 402-412.
7) Ryan JJ, Prochownik E, Gottlieb CA, Apel IJ, Merino R, Nunez G, Clarke MF. C-myc and bcl-2 modulate p53 function by altering p53 subcellular trafficking during the cell cycle. Proc Natl Acad Sci U S A 1994; 91: 5878-5882.
8) Miller DM, Thomas SD, Islam A, Muench D, Sedoris K. C-Myc and cancer metabolism. Clin Cancer Res 2012; 18: 5546-5553.
9) Dang CV, O'Donnell KA, Zeller KI, Nguyen T, Osthus RC, Li F. The c-Myc target gene network. Semin Cancer Biol 2006; 16: 253-264.
10) Toyoshima M, Howie HL, Imakura M, Walsh RM, Annis JE, Chang AN, Frazier J, Chau BN, Loboda A, Linsley PS, Cleary MA, Park JR, Grandori C. Functional genomics identifies therapeutic targets for MYC-driven cancer. Proc Natl Acad Sci U S A 2012; 109: 9545-9550.
11) Hemann MT, Bric A, Teruya-Feldstein J, Herbst A, Nilsson JA, Cordon-Cardo C, Cleveland JL, Tansey WP, Lowe SW. Evasion of the p53 tumour surveillance network by tumour-derived MYC mutants. Nature 2005; 436: 807-811.
12) Gordan JD, Lal P, Dondeti VR, Letrero R, Parekh KN, Oquendo CE, Greenberg RA, Flaherty KT, Rathmell WK, Keith B, Simon MC, Nathanson KL. HIF-alpha effects on c-Myc distinguish two subtypes of sporadic VHL-deficient clear cell renal carcinoma. Cancer Cell 2008; 14: 435-446.
13) Chen C, Chang YC, Liu CL, Chang KJ, Guo IC. Leptin-induced growth of human ZR-75-1 breast cancer cells is associated with up-regulation of cyclin D1 and c-Myc and down-regulation of tumor suppressor p53 and p21WAF1/CIP1. Breast Cancer Res Treat 2006; 98: 121-132.

14) Feldser DM, Kostova KK, Winslow MM, Taylor SE, Cashman C, Whittaker CA, Sanchez-Rivera FJ, Resnick R, Bronson R, Hemann MT, Jacks T. Stage-specific sensitivity to p53 restoration during lung cancer progression. Nature 2010; 468: 572-575.
15) Soucek L, Whitfield J, Martins CP, Finch AJ, Murphy DJ, Sodir NM, Karnezis AN, Swigart LB, Nasi S, Evan GI. Modelling Myc inhibition as a cancer therapy. Nature 2008; 455: 679-683.
16) Li Z, Wu J, Yang D, Zhang L. Large cell carcinoma of lung: analysis of CT signs and review of the literature. The Chinese-German Journal of Clinical Oncology 2006; 5: 309-311.
17) Tomiyama N, Yasuhara Y, Nakajima Y, Adachi S, Arai Y, Kusumoto M, Eguchi K, Kuriyama K, Sakai F, Noguchi M, Murata K, Murayama S, Mochizuki T, Mori K, Yamada K. CT-guided needle biopsy of lung lesions: a survey of severe complication based on 9783 biopsies in Japan. Eur J Radiol 2006; 59: 60-64.
18) Rizzo S, Preda L, Raimondi S, Meroni S, Belmonte M, Monfardini L, Veronesi G, Bellomi M. Risk factors for complications of CT-guided lung biopsies. Radiol Med 2011; 116: 548-563.
19) Fan L, Liu SY, Li QC, Yu H, Xiao XS. Multidetector CT features of pulmonary focal ground-glass opacity: differences between benign and malignant. Br J Radiol 2012; 85: 897-904.
20) Li X, Zhang W, Wu X, Sun C, Chen M, Zeng Q. Mucoepidermoid carcinoma of the lung: common findings and unusual appearances on CT. Clin Imaging 2012; 36: 8-13.